J. Am. Soc. Mass Spectrom. (2015) 26:986–993
DOI: 10.1007/s13361-015-1091-4

RESEARCH ARTICLE

High Resolution Tissue Imaging Using the Single-probe Mass Spectrometry under Ambient Conditions

Wei Rao, Ning Pan, Zhibo Yang

Department of Chemistry and Biochemistry, University of Oklahoma, Norman, Oklahoma 73019, USA

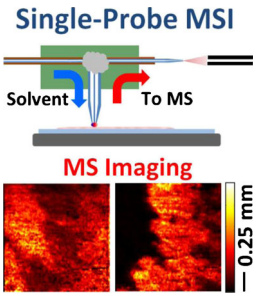

Abstract. Ambient mass spectrometry imaging (MSI) is an emerging field with great potential for the detailed spatial analysis of biological samples with minimal pretreatment. We have developed a miniaturized sampling and ionization device, the Single-probe, which uses in-situ surface micro-extraction to achieve high detection sensitivity and spatial resolution during MSI experiments. The Single-probe was coupled to a Thermo LTQ Orbitrap XL mass spectrometer and was able to create high spatial and high mass resolution MS images at 8±2 and 8.5 μm on flat polycarbonate microscope slides and mouse kidney sections, respectively, which are among the highest resolutions available for ambient MSI techniques. Our proof-of-principle experiments indicate that the Single-probe MSI technique has the potential to obtain ambient MS images with very high spatial resolutions with minimal sample preparation, which opens the possibility for subcellular ambient tissue MSI to be performed in the future.

Keywords: Single-probe MS, High spatial resolution MS imaging, Ambient MS imaging of biological tissues, Liquid surface micro-extraction

Received: 13 November 2014/Revised: 25 January 2015/Accepted: 3 February 2015/Published Online: 25 March 2015

Introduction

Mass spectrometry imaging (MSI) has become an important field in recent years within mass spectrometry (MS) analysis since the first description of matrix assisted laser desorption ionization (MALDI) MSI by Caprioli et al. in 1997 [1]. MSI involves the gathering of MS spectra in a spatially defined manner for a particular sample of interest such that the distribution of a large number of biochemicals such as metabolites and proteins can be obtained within a single experiment. The potential of MSI to improve analysis of biological samples has already been demonstrated in many previous studies, such as the ability to image metabolite distributions in mouse brain sections [2], determine tissue type in tumors [3], to image protein localizations in formalin fixed tissues [4], biomarker discovery [5], and many others.

There has been a variety of different MSI techniques developed over the past decade that have pushed the boundaries of the field in terms of the sensitivity, spatial resolution, and diversity of samples can be analyzed. These techniques can be broadly categorized into nonambient- and ambient-based MSI. The most important nonambient-based methods are MALDI MS [6] and time-of-flight secondary ion MS (ToF-SIMS) [7], which generally have excellent spatial resolution and sensitivity. MALDI MS uses a laser to create gas-phase ions after the sample is treated with matrix molecules and is capable of spatial resolutions of around 5–10 μm, with experiments on tissue routinely performed at a resolution of 50–200 μm [8, 9]. ToF-SIMS uses sputtering ion beam to create secondary ions from the sample surface, and it is able to produce the highest spatial resolution MS images (less than 700 nm for biological samples [10]) but creates fragmented ions because of the high energies involved [11]. However, both of these nonambient techniques generally require the samples to be present in vacuum, and MALDI MS also needs extensive sample pretreatment to work; these inherent drawbacks can potentially compromise sample integrity, leading to a less ideal analysis of biological samples.

Mass spectrometry in the ambient environment has been a relatively recent advancement in the field, with liquid microjunction surface sampling (LMJ-SSP) [12], desorption electrospray ionization (DESI) [13], and direct analysis in real time (DART) [14] being some of the earliest examples. MSI under ambient conditions was first described in 2004 by Takats et al. [13] and has quickly become an important emerging field within mass spectrometry. Ambient MSI methods are capable

Electronic supplementary material The online version of this article (doi:10.1007/s13361-015-1091-4) contains supplementary material, which is available to authorized users.

Correspondence to: Zhibo Yang; *e-mail:* zhibo.yang@ou.edu

of producing MS images with minimal sample preparation and does not require the presence of a vacuum to function, allowing biological samples to be imaged in a near native condition, which is a major advantage over the other nonambient-based techniques. Since then, a number of other ambient MSI modalities have also been developed that utilize different ambient ionization techniques to create MS images. The variety of methods include laser-based techniques such as laser ablation electrospray ionization (LAESI) MS [15] and transmission geometry laser ablation MSI [16], spray-based techniques such as DESI MS and electrostatic spray ionization (ESTASI) MS [17], and surface micro-extraction-based methods such as LMJ-SSP MS [18], liquid extraction surface analysis (LESA) MS [19], and nano-DESI MS [20], among many other emerging technologies that are actively being researched at the present time [21].

LAESI utilizes a mid-IR laser beam to ablate target surfaces, and the produced particles are ionized by the charged liquid droplets from an ESI source. The resolution can reach 200 μm on mouse brain sections [15]. Transmission geometry laser ablation MSI uses a laser to ablate material from a surface into a liquid vortex capture probe that is coupled with the ESI source of a mass spectrometer. The resolution achievable with this method is around 50 μm on a mouse brain section [16]. The DESI method sprays charged solvent droplets at the sample surface to generate the secondary ions detected by MS analysis, and it has been able to achieve a spatial resolution of 35 μm [22] on biological tissues. However, DESI has some drawbacks, including low sensitivity and low ionization efficiency compared with surface extraction-based techniques, which can limit its applications [11]. ESTASI MS uses a high voltage to create localized spray of ions from the sample surface that has been able to achieve a resolution of 200 μm on cell culture samples [17]. Surface micro-extraction techniques, in general, allow a greater efficiency of analyte extraction than spray-based techniques because of a greater efficiency of analyte transfer from the sample to the MS, as has been demonstrated previously where surface digested proteins analyzed with LESA MS were able to give better sensitivity and protein identification than DESI MS [23]. In LMJ-SSP, a liquid micro-extraction junction is formed at the tip of the probe to dissolve analytes on surfaces [18]. The probe consists of two coaxial tubes: one tube provides solvent and the other tube collects and injects the analyte-containing solution to the ionization source, usually electrospray ionization (ESI). This technique provides soft sampling and ionization processes and is not used routinely for MSI experiments attributable to a low spatial resolution (~0.5 mm) [24]. LESA MS creates a micro-extraction junction by suspending a droplet of solvent onto the sample surface, which is capable of direct detection of proteins from human liver samples [25], but suffers from the same spatial resolution problems as LMJ-SSP. Nano-DESI is another type of surface micro-extraction-based soft sampling and ionization method providing high-resolution (~12 μm) measurement without sample preparation [20]. The nano-DESI probe consists of two separate fused silica capillaries: one is to supply the solvent (e.g., methanol/water solution) and the other acts as an ionization emitter to generate ions for MS analysis; the liquid junction formed between the two capillaries samples the analytes present on the sample surface. Despite its powerful features and abilities, nano-DESI suffers from one major problem that has limited its wide-spread use in MSI studies, namely, the difficulty in manipulating the image probe to obtain an optimal interaction between the probe and the sample.

Here, we introduce an improved ambient MSI method based on surface micro-extraction named the Single-probe. The Single-probe has been previously used for the direct analysis of individual cells, which was able to detect the anticancer drugs, cellular lipids, and adenosine phosphates (i.e., AMP, ADP, and ATP) in individual cervical cancer cells (HeLa) [26]. We show here that the Single-probe can be adapted to perform MSI with high surface extraction efficiency at high mass resolution from complex biological samples in the ambient environment with minimal sample preparation, with MS images that have among the highest spatial resolution available from ambient MSI techniques.

Experimental

Chemicals

Water and methanol were purchased as MS grade from Sigma-Aldrich (St. Louis, MO, USA).

Sample Preparation

Rhodamine patterns were produced by using a red Sharpie marker (Sharpie, Downers Grove, Il, USA) to print G1500HS grids (Ted Pella Inc., Redding, CA, USA) onto polycarbonate microscope slides (P11011P; Science Supply Solutions, Elk Grove Village, IL, USA). Mouse brain samples were generously donated by Dr. Mooberry of the University of Texas Health Science Center at San Antonio, and mouse kidney samples were generously donated by Dr. Mao of the University of Oklahoma. Mouse brain and kidney tissues were embedded in optimum cutting temperature compound (Tissue-Tek; Sakura Finetek USA, Torrance, CA, USA) and sectioned at 10 μm thickness using a cryotome at –15°C before mounting onto an indium-tin oxide coated glass slide (Nanocs Inc., New York, NY, USA). The finished slides were dried in air and stored at –80°C before usage. The optical images of the brain slice were taken using PathScan Enabler IV histology slide scanner (Meyer Instruments, Inc. Houston, TX, USA).

Single-probe Fabrication

The Single-probe (Figure 1a) consists of a dual-bore quartz needle, a fused silica capillary, and a nano-electrospray (nano-ESI) emitter. The dual-bore quartz needle was manufactured by pulling a dual-bore quartz capillary (o.d. 500 μm; i.d. 127 μm; Friedrich and Dimmock, Inc., Millville, NJ, USA) using a Sutter P-2000 laser puller (Sutter Instrument, Novato, CA, USA) to achieve a tapered tip. Two fused silica capillaries (o.d. 105 μm, i.d. 40 μm Polymicro Technologies, Phoenix,

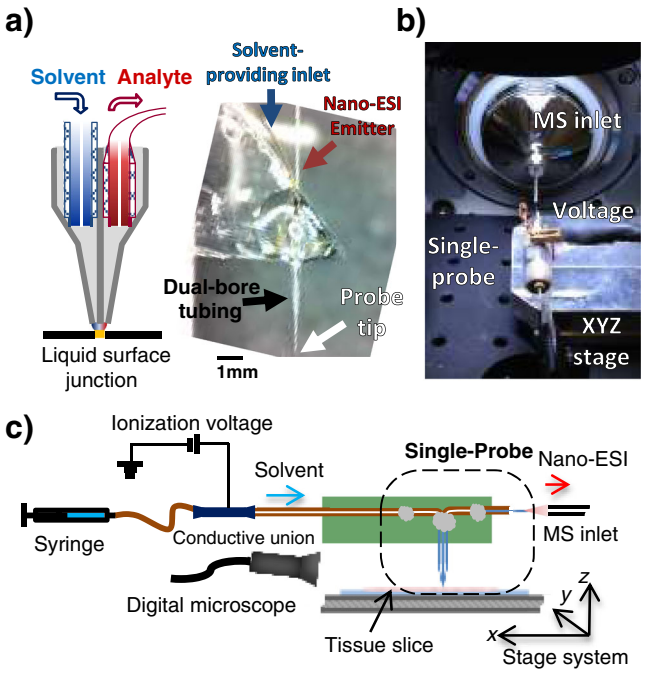

Figure 1. (**a**) Diagram and photograph of the Single-probe showing the various features of the device. (**b**) Photography of the general setup of the Single-probe during MSI measurement. (**c**) Schematic of the Single-probe MSI system

AZ, USA) were threaded inside both of the channels of the pulled Single-probe, and one provides the sampling solvent whereas the other one acts as the nano-ESI emitter, which was secured using UV activated bonding resin (Light Cure Bonding Adhesive; Prime-Dent, Chicago, IL, USA). The unit was mounted onto a glass slide substrate using epoxy that can be conveniently used for MSI experiments (Figure 1a).

MS Imaging and Data Interpretation

During MSI measurement, the sample was placed onto a motorized XYZ stage controlled by a custom designed LabVIEW software developed by the Laskin Group [27]. For rhodamine pattern MSI measurement, the scanning parameters were set to 2 μm/s rastering speed and 5 μm distance between lines. For mouse brain sections the parameters were 12.5 μm/s rastering speed and 25 μm distance between lines. For mouse kidney sections the parameters were 10.0 μm/s rastering speed and 20 μm distance between lines. The MS spectra were acquired using a Thermo LTQ Orbitrap XL mass spectrometer (Figure 1b). For the rhodamine pattern and mouse brain sections, the following parameters were used: mass resolution 30,000 (m/Δm), 5 kV positive mode, 1 microscan, 550 ms max injection time, automatic gain of control (AGC) off. For the mouse kidney sections the following parameters were used: mass resolution 60,000 (m/Δm), 5 kV positive mode, 1 microscan, 150 ms max injection time, AGC on. The solvent used was methanol:water (9:1) supplied at a flow rate of 0.2 μL/min. After data acquisition, the raw MS files were converted to MS images using the MSI QuickView software developed by PNNL [28].

Higher-energy Collisional Dissociation (HCD) MS/MS of Metabolites

The Single-probe was advanced to the surface of the brain section by gradually lifting the Z-stage so that stable ion signals of surface analytes were obtained. HCD MS/MS was then performed with the following parameters on targeted metabolites: mass resolution 60,000 (m/Δm), 5 kV positive mode, 1 microscan, 100 ms injection time, AGC on, activation type HCD, isolation width *m/z* 1.0 (*m/z*±0.5 window), normalized collision energy 30, activation Q 0.25, activation time 30 ms.

Results and Disscussion

Single-probe Properties

The Single-probe device has previously been used for single cell MS analysis [26]. The name "Single-probe" was given because of its integrated design with multiple functions for versatile applications. This device is an integrated unit that is composed of three components: one dual-bore quartz needle, one capillary, and one nano-ESI emitter. This single device has multiple functions capable of probing target, extracting analytes, and ionizing sampled molecules for MS analysis. We have so far utilized this device for several different applications, including MS single cell analysis [26], MS imaging of biological tissues, and detection of fragile sulfated peptides (ongoing research). In MSI measurements, the Single-probe uses surface extraction for sampling, in which a small liquid junction is formed between two bores at the Single-probe tip, for the direct in-situ ambient MSI analysis of samples. By advancing the Single-probe tip closely above the sample surface, a micro-extraction takes place at the tip of the probe. The continuous flow of sampling solvent produces a consistent fresh liquid junction at the probe tip, allowing for constant extraction of analytes present on the surface. The analytes sampled by the micro-junction are then drawn by capillary action towards the nano-ESI emitter. A voltage was conveniently applied to the solvent through the conductive union so that the analytes from the emitter are ionized and introduced into the mass spectrometer using a similar mechanism to ESI (Figure 1c). The sampling and ionization mechanism of the Single-probe MSI technique is similar to those of nano-DESI [29] and LMJ-SSP [18] techniques, in which the liquid junction formed between the orifices of two capillaries performs surface sampling followed by ESI. The integrated design of the Single-probe likely allows for the establishment of relatively easy fabrication protocols and routine operations. Particularly, because of the small size of the tip (<10 μm), which is also the key for single cell MS analysis [24], we can create a micrometer-scale liquid junction to sample the analyte on a much smaller target than was previously possible. We have carried out systematic tests to improve the design of the Single-probe for

conducting robust MSI experiments. The nano-ESI emitter part was made to be as short as possible (typically around 6 mm from the tip of the probe to the end), which in conjunction with the thin fused silica capillary was able to reduce the dead volume to around 3 nL and minimize the effects of sample carryover. The reduced dead volume inside of the nano-ESI emitter resulted in a minimized delay time (<1 s) between surface contact and MS detection.

Single-probe MSI for Rhodamine Grid on Flat Surface

We have fabricated the Single-probes with small tip size (<10 μm) to characterize their capability of obtaining high spatial resolution MSI. The maximum spatial resolution of the Single-probe was obtained by using a small tip (e.g., 6.0 μm, Figure 2a) rastering across a surface area covered with rhodamine. Further reducing the tip size (e.g., <5 μm) will result in frequent clogging in the Single-probe and interruption of the experiment. Rhodamine is routinely used as a standard for solvent-based ambient MSI because of its ease of ionization under ambient conditions [20, 30]. The Single-probe was able to produce a trace on the Rhodamine surface with a width of 4.9 μm (Figure 2b), which was achieved as the area of surface contact was smaller than the Single-probe tip diameter (6.0 μm). MSI was also performed on a Rhodamine pattern, printed using a standard G1500HS transmission electron microscopy (TEM) grid, on a polycarbonate microscope slide (Figure 2c). The Single-probe was able to produce MS images with high spatial resolution for a species found at *m/z* 457.94 (Figure 2d), with the image fidelity well maintained over a relatively large area (150×100 μm, Supplementary Figure S1). The maximum resolution of the system in MSI mode was estimated to be around 8±2 μm (pixel size is 2.0×5.0 μm), which was based on the rate of increase and decrease in signal around sharp features as suggested by Heeren and co-workers

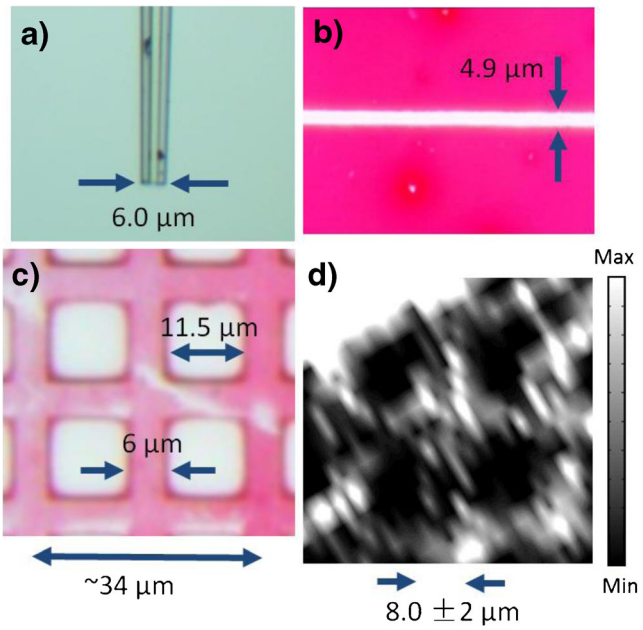

Figure 2. (**a**) Photograph of the Single-probe tip. (**b**) The optical image of the Single-probe trace across rhodamine film deposited on a polycarbonate microscope slide. (**c**) Optical image of rhodamine pattern printed using a G1500HS TEM grid. (**d**) MS image of species at *m/z* 457.94. Note the optical and MS image has been rotated to give a better visual representation of the grid. The original orientation can be seen in Supplementary Figure S1

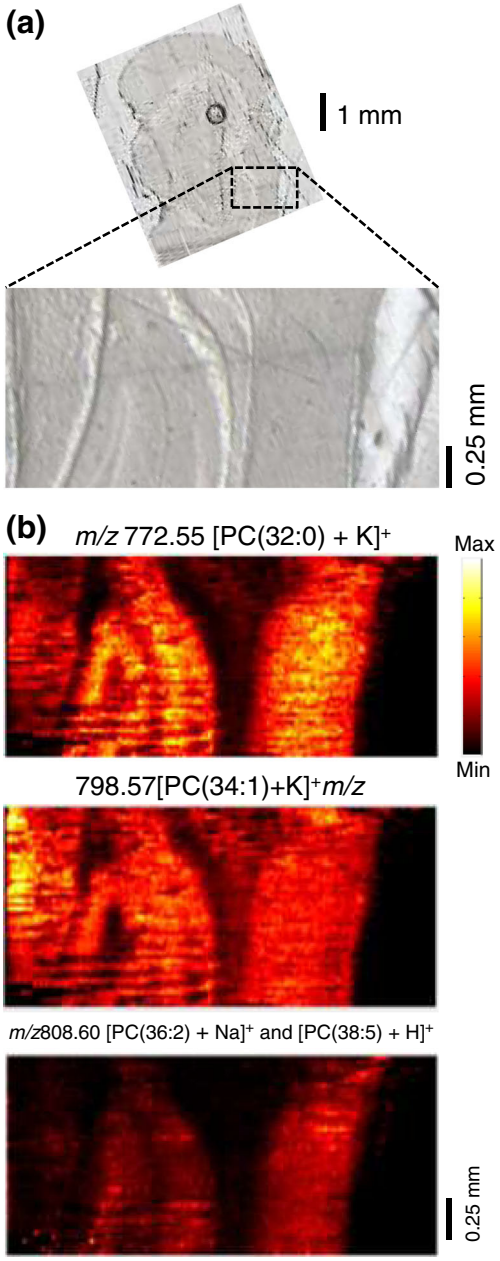

Figure 3. (**a**) Optical image of the mouse brain section showing the region of MSI measurement. (**b**) MS images of various metabolites taken at 12.5×25 μm pixel size with their corresponding *m/z* values, *m/z* 772.55 phosphatidylcholine [(PC) (32:0)+K]$^+$, *m/z* 798.57 [PC (34:1)+K]$^+$, and *m/z* 808.60 [PC (36:2)+Na]$^+$ and [PC (38:5)+H]$^+$

[31]. This demonstrates the ability of the Single-probe to conduct very high spatial resolution MSI on flat surfaces.

High Spatial and Mass Resolution MSI of Mouse Brain Section

High spatial resolution ambient MSI has generally been more difficult to achieve on complex biological samples such as tissue sections, which contains small surface unevenness (e.g., 1.5±0.6 μm variation [27]) that can introduce a greater degree of heterogeneity to data acquisition compared with flat surfaces. DESI MSI of biological samples are routinely made at a resolution of 200 μm [32, 33], which is capable of giving informative analysis of large tissue sections but does not contain details that can be observed at higher spatial resolution. One study with DESI MS was able to achieve a spatial resolution of 35 μm; however, the images were acquired with low mass resolution and with relatively low ion signals [22]. For surface micro-extraction techniques, LMJ-SSP and LESA MS are capable of producing pixel sizes at around 0.5–1 mm

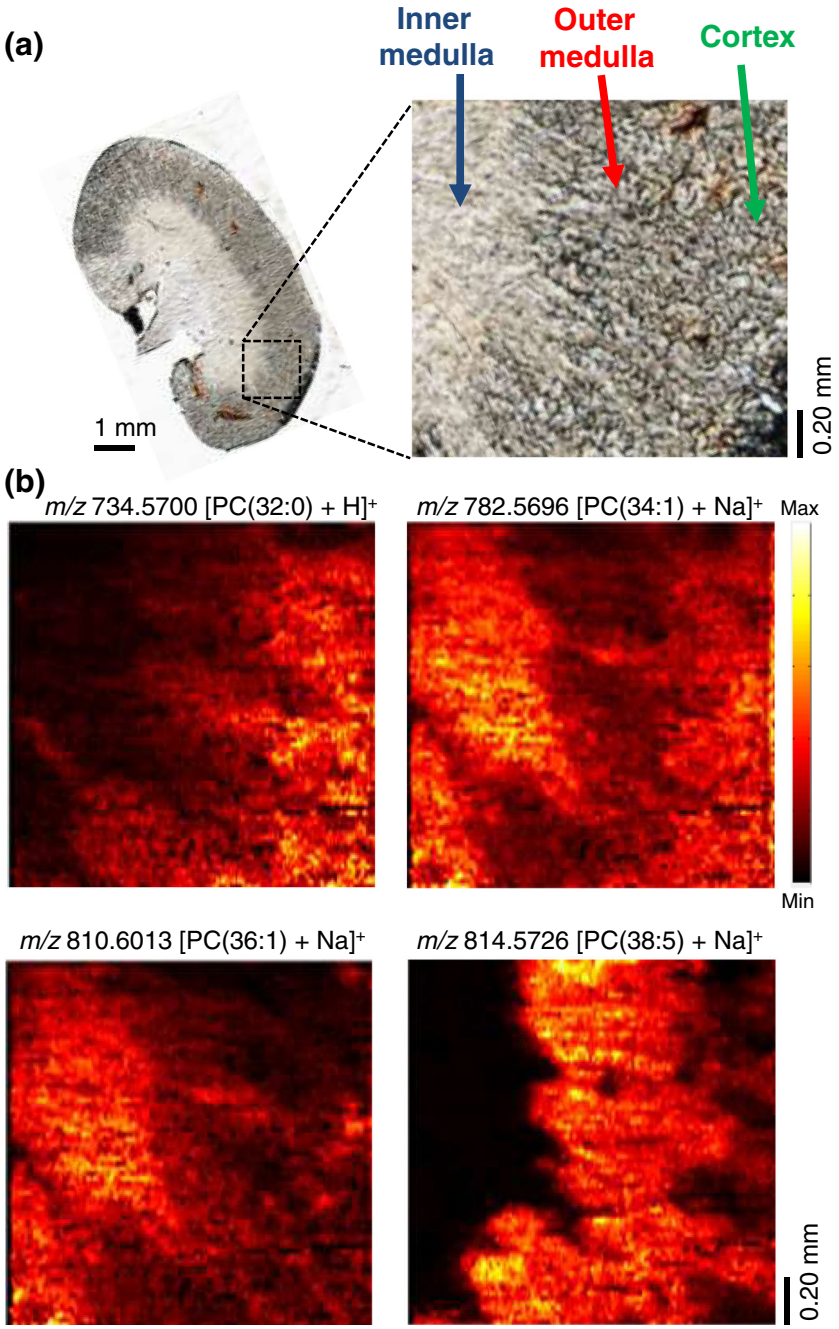

Figure 4. (**a**) Optical image of the mouse kidney section showing the region of MSI measurement. (**b**) MS images of various metabolites taken at 8.5×20 μm pixel size with their corresponding high resolution *m/z* values, *m/z* 734.5700 phosphatidylcholine [(PC) (32:0)+H]$^+$, *m/z* 782.5696 [PC(34:1)+Na]$^+$, *m/z* 810.6013 [PC(36:1)+Na]$^+$, and *m/z* 814.5726 [PC(38:5)+Na]$^+$

because of the nature of the tip size [34]. By using the Single-probe MSI technique, we have obtained images from mouse brain section samples at a resolution of 12.5 μm (pixel size is 12.5×25 μm) (Figure 3), which was verified using the rise or decay of signals across sharp features within the sample [31] for the species *m/z* 772.55 $[PC(32:0)+K]^+$ (Supplementary Figure S2a).

We then applied the Single-probe to the MS imaging of a section of mouse kidney sections. Kidney samples have been the target of MS imaging experiments in the past in MALDI MS [35] and ambient MS imaging [20, 36], where the contrast among the inner medulla, outer medulla, and the cortex make it an excellent target for MS imaging experiments (Figure 4a). The images were acquired at 10 μm/s raster speed with AGC mode on and were made with high mass resolution at 60,000 m/Δm. This technique was shown to have very good surface extraction efficiency with the absolute intensity achieved for surface extraction reaching more than 3.0×10^7 (Figure 5a). The number of scans per line was 188 scans over a period of 160 s. A high spatial resolution (8.5 μm; pixel size is 8.5×20 μm) was obtained based on the ion intensity change of the metabolite $[PC(38:5)+Na]^+$ at *m/z* 814.5726 for the outer medulla (Figure 5b, c, and d) using the method mentioned previously [31]. We further verified the spatial resolution measurement at other two different locations within the sample (Supplementary Figure S2b), and obtained the same result. To the best of our knowledge, 8.5 μm is amongst the highest spatial resolution that has been achieved so far using the ambient ionization MS imaging methods on biological tissues with minimal sample preparation.

Using high accurate mass MS and previously published results [20, 37–39] we were able to identify a number of metabolites, including *m/z* 734.5700 $[PC(32:0)+H]^+$, *m/z* 782.5696 $[PC(34:1)+Na]^+$, and *m/z* 810.6013 $[PC(36:1)+Na]^+$ (Figure 4b) amongst others, with a mass accuracy at less than 4.0 ppm (Table S1). We were also able to validate the identifications by subjecting the metabolites to higher-energy collisional dissociation (HCD) MS/MS analysis at 60,000 (m/Δm) mass resolution with a *m/z* ±0.5 window. Figure 6a shows the MS/MS spectrum for *m/z* 798.5467, which contains the characteristic peak at *m/z* 162.9566 corresponding to the potassium adduct of $CH_3CH_2PO_4$ ($[CH_3CH_2PO_4+K]^+$) and

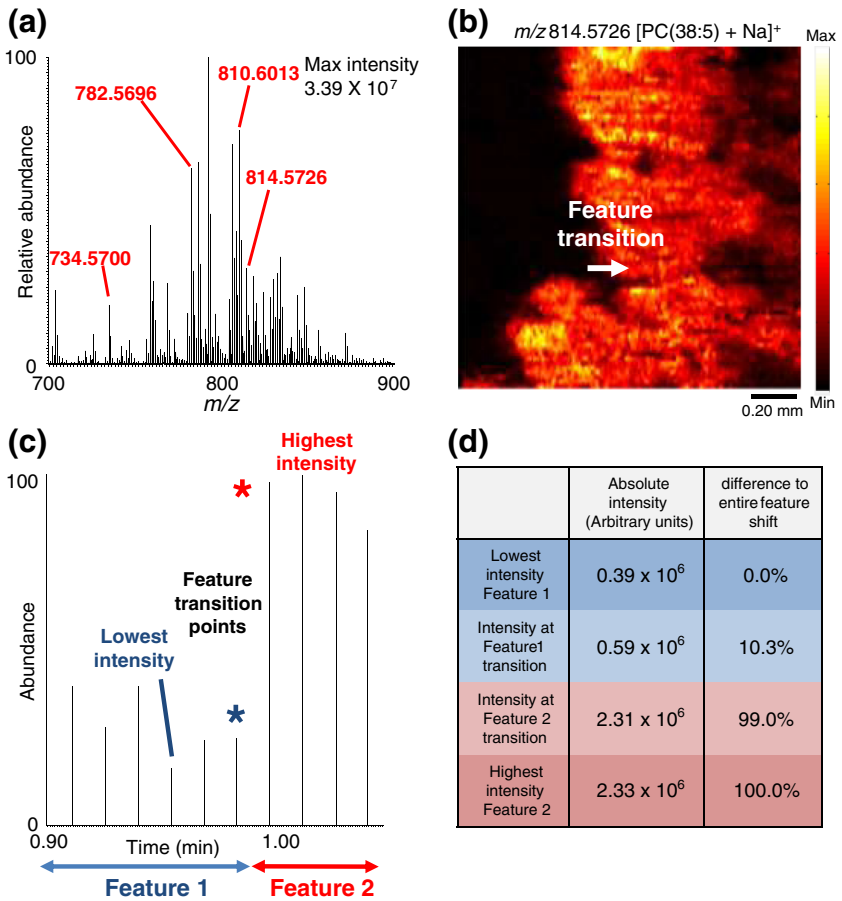

	Absolute intensity (Arbitrary units)	difference to entire feature shift
Lowest intensity Feature 1	0.39×10^6	0.0%
Intensity at Feature1 transition	0.59×10^6	10.3%
Intensity at Feature 2 transition	2.31×10^6	99.0%
Highest intensity Feature 2	2.33×10^6	100.0%

Figure 5. (**a**) Typical mass spectrum of metabolites found by surface extraction of mouse brain sections. The highest sensitivity was generally reached at above 3.0×10^7. (**b**) Feature transition point for testing of resolution for $[PC(38:5)+Na]^+$ (*m/z* 814.5726). (**c**) The chronogram for the intensities at the transition point between the inner medulla and the outer medulla for *m/z* 814.5726. (**d**) The mass spectral intensities for *m/z* 814.5726 at the transition points compared with the lowest and highest intensities for before and after the transition, and the measured spatial resolution is 8.5 μm

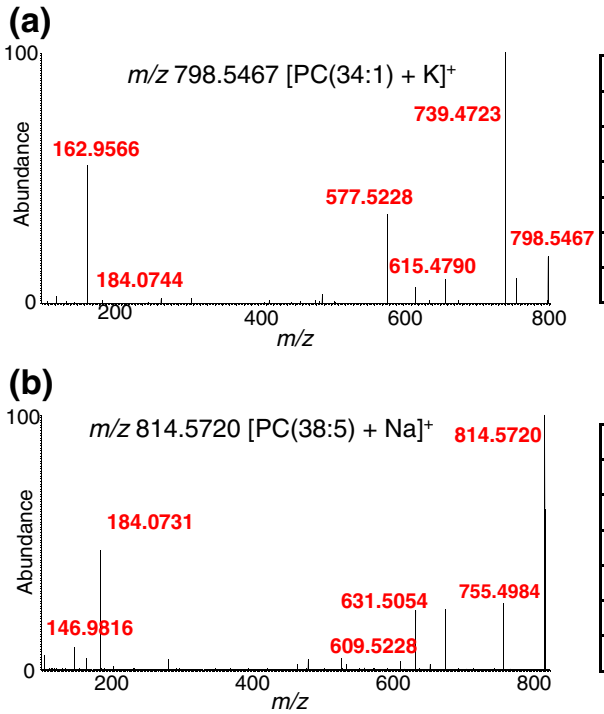

m/z	Product ion
798.5467	$[M + K]^+$
739.4723	$[M+ K – N(CH_3)_3]^+$
615.4790	$[M + K – HOPO_3(CH_2)_2N(CH_3)_3]^+$
577.5228	$[M + K – KOPO_3(CH_2)_2N(CH_3)_3]^+$
184.0744	$[HOPO_3(CH_2)_2N(CH_3)_3+ H]^+$
162.9566	$[CH_3CH_2PO_4+ K]^+$

m/z	Product ion
814.5720	$[M + Na]^+$
755.4984	$[M + Na – N(CH_3)_3]^+$
631.5054	$[M + Na – HOPO_3(CH_2)_2N(CH_3)_3]^+$
609.5228	$[M + Na – NaOPO_3(CH_2)_2N(CH_3)_3]^+$
184.0731	$[HOPO_3(CH_2)_2N(CH_3)_3+ H]^+$
146.9816	$[CH_3CH_2PO_4+ Na]^+$

Figure 6. HCD MS/MS fragmentation of (**a**) *m/z* 798.5467 [PC (34:1)+K]$^+$ and (**b**) *m/z* 814.5720 [PC (38:5)+Na]$^+$. Characteristic *m/z* differences are observed in the fragments for the K^+ and Na^+ adduct ions

neutral losses of *m/z* 59.0744 for $N(CH_3)_3$ (at *m/z* 739.4723) and *m/z* 221.0239 for $KOPO_3(CH_2)_2N(CH_3)_3$ (at *m/z* 577.5228), indicating that the parent ion at *m/z* 798.5467 is [PC (34:1)+K]$^+$. The fragment at *m/z* 184.0744 corresponding to the PC head group $[HOPO_3(CH_2)_2N(CH_3)_3+H]^+$ was observed at low intensities, and this fragment was observed previously for both protonated species and metal ion adducts of certain PCs [40]. For the MS/MS spectrum at *m/z* 814.5720 (Figure 6b) the characteristic peak at *m/z* 146.9822 indicates the presence of the sodium adduct by the presence of the $[CH_3CH_2PO_4+Na]^+$ fragment ion, with neutral losses of *m/z* 59.0739 for $N(CH_3)_3$ (at *m/z* 755.4984) and *m/z* 205.0494 for $NaOPO_3(CH_2)_2N(CH_3)_3$ (at *m/z* 609.5228) are indications the presence of [PC (38:5)+Na]$^+$. Mass assignments were also validated for a number of other metabolites that were found on the surface of the mouse tissue sections during Single-probe MSI (Supplementary Figure S3).

Conclusion

We have introduced the Single-probe MSI, which is capable of producing high spatial and mass resolution MS images from complex biological samples under ambient conditions. The best spatial resolution achieved so far on biological tissues is 8.5 µm, which is amongst the highest yet achieved from ambient MSI techniques with minimal sample preparation on complex biological samples. The tip size and shape are crucial factors in improving spatial resolution by creating a better and more robust surface micro-extraction junction during MSI, and probes can be made to potentially create images at a cellular resolution. This level of resolution would allow even more detailed features to be observed for ambient MSI, and we hope to eventually use the Single-probe to create MS images at subcellular levels. Statistical imaging techniques such as imaging multivariate analysis (MVA) [41] may also be used in the future with our MS images to further improve data interpretation and allow automated feature identification to be made. The Single-probe has the potential to offer great improvements in the field of ambient MS imaging that can lead to a better understanding of biological systems and diseases.

Acknowledgments

The authors thank Dr. Laskin at the Pacific Northwest National Laboratory for the use of the LabVIEW software for controlling the XYZ stage as well as the use of the MSI QuickView program for visualizing MS images developed in her lab. The authors thank Dr. Mooberry at the University of Texas Health Science Center at San Antonio for providing the mouse brain sections for MSI analysis. They also thank Dr. Liu and Dr. Mao at the University of Oklahoma for the use of the laser puller in the manufacturing of the probe, and for providing the mouse kidney sections for MSI analysis, respectively. This research was supported by grants from the Research Council of the University of Oklahoma Norman Campus, the American Society for Mass Spectrometry Research Award (sponsored by Waters Corporation), and Oklahoma Center for the Advancement of Science and Technology (grant HR 14-152).

References

1. Caprioli, R.M., Farmer, T.B., Gile, J.: Molecular imaging of biological samples: localization of peptides and proteins using MALDI-TOF MS. Anal. Chem. **69**, 4751–4760 (1997)
2. Lanekoff, I., Thomas, M., Carson, J.P., Smith, J.N., Timchalk, C., Laskin, J.: Imaging nicotine in rat brain tissue by use of nanospray desorption electrospray ionization mass spectrometry. Anal. Chem. **85**, 882–889 (2013)
3. Gerbig, S., Golf, O., Balog, J., Denes, J., Baranyai, Z., Zarand, A., Raso, E., Timar, J., Takats, Z.: Analysis of colorectal adenocarcinoma tissue by desorption electrospray ionization mass spectrometric imaging. Anal. Bioanal. Chem. **403**, 2315–2325 (2012)
4. Casadonte, R., Caprioli, R.M.: Proteomic analysis of formalin-fixed paraffin-embedded tissue by MALDI imaging mass spectrometry. Nat. Protoc. **6**, 1695–1709 (2011)
5. Schwamborn, K.: Imaging mass spectrometry in biomarker discovery and validation. J. Proteome. **75**, 4990–4998 (2012)
6. Schwamborn, K., Caprioli, R.M.: MALDI imaging mass spectrometry - painting molecular pictures. Mol. Oncol. **4**, 529–538 (2010)
7. Brunelle, A., Laprevote, O.: Lipid imaging with cluster time-of-flight secondary ion mass spectrometry. Anal. Bioanal. Chem. **393**, 31–35 (2009)
8. Rompp, A., Spengler, B.: Mass spectrometry imaging with high resolution in mass and space. Histochem. Cell Biol. **139**, 759–783 (2013)
9. Yang, J., Caprioli, R.M.: Matrix sublimation/recrystallization for imaging proteins by mass spectrometry at high spatial resolution. Anal. Chem. **83**, 5728–5734 (2011)
10. Brison, J., Robinson, M.A., Benoit, D.S.W., Muramoto, S., Stayton, P.S., Castner, D.G.: TOF-SIMS 3D imaging of native and non-native species within HeLa cells. Anal. Chem. **85**, 10869–10877 (2013)
11. Vickerman, J.C.: Molecular imaging and depth profiling by mass spectrometry—SIMS, MALDI or DESI? Analyst **136**, 2199–2217 (2011)
12. Van Berkel, G.J., Sanchez, A.D., Quirke, J.M.: Thin-layer chromatography and electrospray mass spectrometry coupled using a surface sampling probe. Anal. Chem. **74**, 6216–6223 (2002)
13. Takats, Z., Wiseman, J.M., Gologan, B., Cooks, R.G.: Mass spectrometry sampling under ambient conditions with desorption electrospray ionization. Science **306**, 471–473 (2004)
14. Cody, R.B., Laramee, J.A., Durst, H.D.: Versatile new ion source for the analysis of materials in open air under ambient conditions. Anal. Chem. **77**, 2297–2302 (2005)
15. Nemes, P., Woods, A.S., Vertes, A.: Simultaneous imaging of small metabolites and lipids in rat brain tissues at atmospheric pressure by laser ablation electrospray ionization mass spectrometry. Anal. Chem. **82**, 982–988 (2010)
16. Ovchinnikova, O.S., Bhandari, D., Lorenz, M., Van Berkel, G.J.: Transmission geometry laser ablation into a non-contact liquid vortex capture probe for mass spectrometry imaging. Rapid Commun. Mass Spectrom. **28**, 1665–1673 (2014)
17. Qiao, L., Tobolkina, E., Lesch, A., Bondarenko, A., Zhong, X., Liu, B., Pick, H., Vogel, H., Girault, H.H.: Electrostatic spray ionization mass spectrometry imaging. Anal. Chem. **86**, 2033–2041 (2014)
18. Van Berkel, G.J., Kertesz, V., Koeplinger, K.A., Vavrek, M., Kong, A.N.: Liquid microjunction surface sampling probe electrospray mass spectrometry for detection of drugs and metabolites in thin tissue sections. J. Mass Spectrom. **43**, 500–508 (2008)
19. Kertesz, V., Van Berkel, G.J.: Fully automated liquid extraction-based surface sampling and ionization using a chip-based robotic nanoelectrospray platform. J. Mass Spectrom. **45**, 252–260 (2010)
20. Laskin, J., Heath, B.S., Roach, P.J., Cazares, L., Semmes, O.J.: Tissue imaging using nanospray desorption electrospray ionization mass spectrometry. Anal. Chem. **84**, 141–148 (2012)
21. Wu, C., Dill, A.L., Eberlin, L.S., Cooks, R.G., Ifa, D.R.: Mass spectrometry imaging under ambient conditions. Mass Spectrom. Rev. **32**, 218–243 (2012)
22. Campbell, D.I., Ferreira, C.R., Eberlin, L.S., Cooks, R.G.: Improved spatial resolution in the imaging of biological tissue using desorption electrospray ionization. Anal. Bioanal. Chem. **404**, 389–398 (2012)
23. Rao, W., Celiz, A.D., Scurr, D.J., Alexander, M.R., Barrett, D.A.: Ambient DESI and LESA-MS analysis of proteins adsorbed to a biomaterial surface using in-situ surface tryptic digestion. J. Am. Soc. Mass Spectrom. **24**, 1927–1936 (2013)
24. Van Berkel, G.J., Kertesz, V.: Continuous-flow liquid microjunction surface sampling probe connected on-line with high-performance liquid chromatography/mass spectrometry for spatially resolved analysis of small molecules and proteins. Rapid Commun. Mass Spectrom. **27**, 1329–1334 (2013)
25. Sarsby, J., Martin, N.J., Lalor, P.F., Bunch, J., Cooper, H.J.: Top-down and bottom-up identification of proteins by liquid extraction surface analysis mass spectrometry of healthy and diseased human liver tissue. J. Am. Soc. Mass Spectrom. **25**, 1953–1961 (2014)
26. Pan, N., Rao, W., Kothapalli, N.R., Liu, R., Burgett, A.W.G., Yang, Z.: The Single-probe: a miniaturized multifunctional device for single cell mass spectrometry analysis. Anal. Chem. **86**, 9376–9380 (2014)
27. Lanekoff, I., Heath, B.S., Liyu, A., Thomas, M., Carson, J.P., Laskin, J.: Automated platform for high-resolution tissue imaging using nanospray desorption electrospray ionization mass spectrometry. Anal. Chem. **84**, 8351–8356 (2012)
28. Thomas, M., Heath, B.S., Laskin, J., Li, D.S., Liu, E., Hui, K., Kuprat, A.P., van Dam, K.K., Carson, J.P.: Visualization of high resolution spatial mass spectrometric data during acquisition. 2012 Annual International Conference of the IEEE Engineering in Medicine and Biology Society (EMBC), San Diego, CA, USA, Aug 28th to Sept 1st, 5545–5548 (2012)
29. Roach, P.J., Laskin, J., Laskin, A.: Nanospray desorption electrospray ionization: an ambient method for liquid-extraction surface sampling in mass spectrometry. Analyst **135**, 2233–2236 (2010)
30. Kertesz, V., Van Berkel, G.J.: Improved imaging resolution in desorption electrospray ionization mass spectrometry. Rapid Commun. Mass Spectrom. **22**, 2639–2644 (2008)
31. Luxembourg, S.L., Mize, T.H., McDonnell, L.A., Heeren, R.M.: High-spatial resolution mass spectrometric imaging of peptide and protein distributions on a surface. Anal. Chem. **76**, 5339–5344 (2004)
32. Eberlin, L.S., Ferreira, C.R., Dill, A.L., Ifa, D.R., Cooks, R.G.: Desorption electrospray ionization mass spectrometry for lipid characterization and biological tissue imaging. Biochim. Biophys. Acta Mol. Cell Biol. Lipids **1811**, 946–960 (2011)
33. Eberlin, L.S., Norton, I., Orringer, D., Dunn, I.F., Liu, X.H., Ide, J.L., Jarmusch, A.K., Ligon, K.L., Jolesz, F.A., Golby, A.J., Santagata, S., Agar, N.Y.R., Cooks, R.G.: Ambient mass spectrometry for the intraoperative molecular diagnosis of human brain tumors. Proc. Natl. Acad. Sci. U. S. A. **110**, 1611–1616 (2013)
34. Eikel, D., Vavrek, M., Smith, S., Bason, C., Yeh, S., Korfmacher, W.A., Henion, J.D.: Liquid extraction surface analysis mass spectrometry (LESA-MS) as a novel profiling tool for drug distribution and metabolism analysis: the terfenadine example. Rapid Commun. Mass Spectrom. **25**, 3587–3596 (2011)
35. Marsching, C., Eckhardt, M., Grone, H.J., Sandhoff, R., Hopf, C.: Imaging of complex sulfatides SM3 and SB1a in mouse kidney using MALDI-TOF/TOF mass spectrometry. Anal. Bioanal. Chem. **401**, 53–64 (2011)
36. Janfelt, C., Wellner, N., Hansen, H.S., Hansen, S.H.: Displaced dual-mode imaging with desorption electrospray ionization for simultaneous mass spectrometry imaging in both polarities and with several scan modes. J. Mass Spectrom. **48**, 361–366 (2013)
37. Girod, M., Shi, Y., Cheng, J.X., Cooks, R.G.: Desorption electrospray ionization imaging mass spectrometry of lipids in rat spinal cord. J. Am. Soc. Mass Spectrom. **21**, 1177–1189 (2010)
38. Dill, A.L., Ifa, D.R., Manicke, N.E., Ouyang, Z., Cooks, R.G.: Mass spectrometric imaging of lipids using desorption electrospray ionization. J. Chromatogr. B Analyt. Technol. Biomed. Life Sci. **877**, 2883–2889 (2009)
39. Lanekoff, I., Burnum-Johnson, K., Thomas, M., Short, J., Carson, J.P., Cha, J., Dey, S.K., Yang, P., Prieto Conaway, M.C., Laskin, J.: High-speed tandem mass spectrometric in situ imaging by nanospray desorption electrospray ionization mass spectrometry. Anal. Chem. **85**, 9596–9603 (2013)
40. Pridmore, C.J., Mosely, J.A., Sanderson, J.M.: The reproducibility of phospholipid analyses by MALDI-MSMS. Analyst **136**, 2598–2605 (2011)
41. Rao, W., Scurr, D.J., Burston, J., Alexander, M.R., Barrett, D.A.: Use of imaging multivariate analysis to improve biochemical and anatomical discrimination in desorption electrospray ionization mass spectrometry imaging. Analyst **137**, 3946–3953 (2012)